A Varactor-Tuned RF Tunable Bandpass Filter with Constant Bandwidth

Byung-Wook Kim · Du-Il Yun · Sang-Won Yun

Abstract

A novel RF tunable bandpass filter structure using dielectric resonators and varactor diodes is considered for the optimization to achieve constant bandwidth with minimum passband insertion loss. The coupling between resonators is realized by coupling windows and series lumped L, C elements are used to realize the input/output stage couplings. A 5 poles, 0.01 dB ripple Chebyshev type filter tuned from 800 MHz~900 MHz is designed and presented in this paper. The passband bandwidth for the design is 10 MHz (fractional bandwidth = 1.2 %). Experimental results show that the 3 dB passband bandwidth variation is 12.04 MHz~12.16 MHz (less than 1 %) and passband insertion loss is 15 dB~7 dB depending on the tuning voltages.

Key words : Tunable bandpass filter, Varactor, Constant bandwidth

Ⅰ. Introduction

Electrically tunable filters have wide application in multiband wireless communication system, spectrum measurement system, and radar system[1]~[5]. The system requirements for these system would be broadband tuning bandwidth, fast tuning time, cost effectiveness, small size, minimum passband insertion loss and constant bandwidth[1]~[6]. Because relatively high Q varactors and RF equalizer[9] are now available, optimally designed varactor-tuned RF bandpass filter would satisfy these system req uirements. 2~4 poles varactor-tuned filters have been previously developed[2]~[5]. However, these results show relatively large passband bandwidth variation, it is because there are no design consideration for the constant passband bandwidth.

Fig. 1 shows varactor-tuned RF bandpass filters considered in this paper. This filter is composed of dielectric resonator and varactor diode. Because low characteristic impedance with high Q can be easily achieved with dielectric resonators, this structure has broadband tuning bandwidth[5]. Also, this structure does not suffered from parasitic components generated at short circuit points of the resonators[3]. Basically, the resonators are designed for high Q operation(i.e. low varactor C, large dielectric resonator length) to minimize passband insertion loss. The couplings between resonators are realized by virtue of coupling windows and the couplings of input/output section are realized by use of series lumped L, C elements. We will show the optimum design method to achieve constant bandwidth with minimum passband insertion loss. And design example will be presented to prove the validity of the proposed design method.

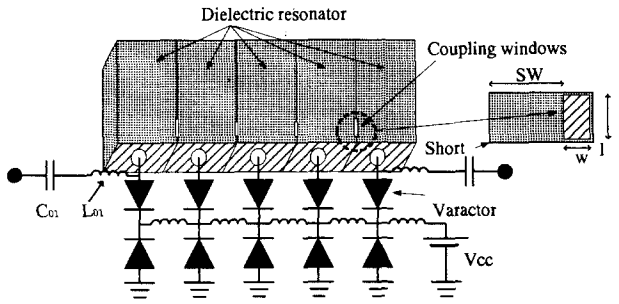

Fig. 1. A novel varactor-tuned RF bandpass filter.

Ⅱ. Analysis of Coupling Windows

Since tunable filters are generally of narrow bandwidth, coupling factor is chosen as basic design parameters[1]. Fig. 2 demonstrates the two poles bandpass filter which can be practically used to measure the coupling factors of the coupling windows. Because input/output capacitive coupling section is located in proximity to the short circuit point of the dielectric resonator, low input/output coupling is introduced. It has been reported[1] that transmission coefficient of Fig. 2 will show two minimum VSWR points because this is so-called "overcoupled case". Let two points be f_1, f_2, then the coupling factor, k, is given as eq. (1)[1].

$$k=\frac{f_2-f_1}{\sqrt{f_2*f_1}} \tag{1}$$

The scattering parameters of the coupling windows shown in Fig. 2 can be approximately calculated by application of Bethe's small aperture theory[7],[8], image theory and Lorentz's reciprocal

Manuscript received October 31, 2001; revised November 27, 2001.

B. W. Kim, D. I. Yun, S. W. Yun is with the Dept. of Electronics Engineering, Sogang University.

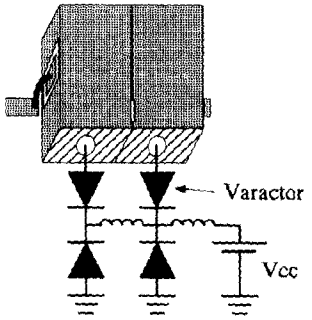

Fig. 2. The configuration for the measurement and the calculation of coupling factor, k.

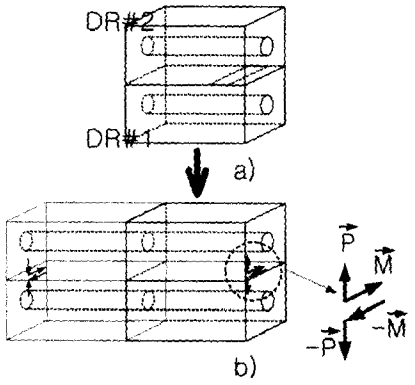

Fig. 3. Equivalent configuration of dielectric resonator with coupling window obtained by application of Bethe's small aperture theory and image theory.

theorem[7]. Consider two dielectric resonators shown in Fig. 2 which can be approximately represented by application of Bethe's small aperture theory and image theory as shown in Fig. 3.

In Bethe's small aperture theory with introduction of reaction terms[7], the dipole moments are related to the normal electric field and tangential magnetic field which can be written as eq. (2) and eq. (3).

$$\vec{P}=-\varepsilon a_e[\vec{n}\cdot\vec{E}_g+\vec{n}\cdot\vec{E}_{1r}-\vec{n}\cdot\vec{E}_{2r}]\vec{n} \tag{2}$$

$$\vec{M}=-a_m[\vec{H}_g+\vec{H}_{1r}-\vec{H}_{2r}]_t \tag{3}$$

where, $\vec{P}$ is electric dipole moment, $\vec{M}$ is magnetic dipole moment, $\vec{E}_g$, $\vec{H}_g$ are the dominant mode fields in the DR(dielectric resonator) #1 in the absence of the aperture, $\vec{E}_{1r}$, $\vec{H}_{1r}$ are the dominant mode fields radiated by the $-\vec{P}$, $-\vec{M}$ in DR #1, $\vec{E}_{2r}$, $\vec{H}_{2r}$ are the dominant mode fields radiated by $\vec{P}$, $\vec{M}$ in DR #2, $\vec{n}$ is unit vector normal to aperture and a_e, a_m are electric polarizability and magnetic polarizability, respectively.

Because we choose rectangular type apertures as coupling windows, it is difficult to calculate a_e and a_m. For this reason, the published results by S. B. Cohn[1],[10] are used.

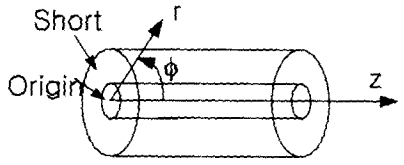

Fig. 4. The coordinate used for calculation.

To reduce the difficulties in calculation, we assume that the structure of DR is perfectly coaxial and lossless one. The coordinate for calculation is selected as shown in Fig. 4.

With these assumptions, $\vec{E}_g$, $\vec{H}_g$ can be expressed as eq. (4) and eq. (5).

$$E_g=\left(C\frac{e^{j\beta z}}{r}-C\frac{e^{-j\beta z}}{r}\right)\vec{a}_r = C\frac{2j\sin\beta z}{r}\vec{a}_r \tag{4}$$

$$H_g=CY_0\frac{-2\cos\beta z}{r}\vec{a}_\phi \tag{5}$$

where, C is the arbitrary amplitude of electric field at open wall of DR #1, $\frac{1}{Y_0}=Z_0=\frac{138}{\sqrt{\varepsilon_r}}\log(1.0787\frac{b}{a})$, β is the propagation constant, a is the inner radius of DR, b is the average outer radius of DR and the coordinates of the position (r,ϕ,z) are as shown in Fig. 4.

Let the position of the dipole moment $\vec{P}$ of DR #2, which is shown in Fig. 3, be $r=b, z=d$ and A_{11}, A_{12} be the amplitudes of electric fields radiated by this dipole moment to +z direction and -z direction, respectively. There are another dipole moment $-\vec{P}$ at $r=b, z=-d$ which is introduced to account for the short point of the DR #2. Let A_{21} be amplitude of the electric field radiated by this dipole moment to +z direction and A_{22} be that to -z direction. $A_{11}, A_{12}, A_{21}, A_{22}$ can be expressed as eq. (6) ~ eq. (9) by Lorentz's reciprocal theorem[7].

$$A_{11}=-\frac{jwP_r}{Pb}e^{j\beta d} \tag{6}$$

$$A_{12}=\frac{jwP_r}{Pb}e^{-j\beta d} \tag{7}$$

$$A_{21}=-A_{12} \tag{8}$$

$$A_{22}=-A_{11} \tag{9}$$

where, P_r is the r component of $\vec{P}$, $P=4\pi Y_0\ln\frac{b}{a}$ and w is radians per second. Similarly, let A_{31}, A_{32} be amplitudes of the electric field radiated by magnetic dipole moment $\vec{M}$ at $r=b, z=d$ to +z direction and -z direction, respectively, and

A_{41}, A_{42} be amplitudes of the electric field radiated by magnetic dipole moment $\vec{M}$ at $r=b, z=-d$ to +z direction and $-z$ direction, respectively. $A_{31}, A_{32}, A_{41}, A_{42}$ can be expressed as eq. (10)~eq. (13).

$$A_{31}=\frac{jw\mu_0 Y_0}{Pb}e^{j\beta d}M_\phi \tag{10}$$

$$A_{32}=\frac{jw\mu_0 Y_0}{Pb}e^{-j\beta d}M_\phi \tag{11}$$

$$A_{41}=-A_{32} \tag{12}$$

$$A_{42}=-A_{31} \tag{13}$$

where, M_ϕ is ϕ component of $\vec{M}$. With these expressions, $\vec{a}_r\cdot(\vec{E}_{1r}-\vec{E}_{2r})$ of eq. (2) can be expressed as

$$\begin{aligned}E_{1rr}-E_{2rr}=&-(A_{11}+A_{12}+A_{31}+A_{32})E^+\cdot\vec{a}_r\\&-(A_{21}+A_{41})E^-\cdot\vec{a}_r\\&-(A_{12}+A_{32})E^+\cdot\vec{a}_r\end{aligned} \tag{14}$$

where, E^+ is the electric field which is traveling to +z direction at $r=b$, $z=d$ and E^- is traveling to $-z$ direction. E^+, E^- can be expressed as

$$E^+=\frac{e^{-j\beta d}}{b}\vec{a}_r \tag{15}$$

$$E^-=\frac{e^{j\beta d}}{b}\vec{a}_r \tag{16}$$

Similarly, $H_{1rr}-H_{2rr}$ can be expressed as

$$\begin{aligned}H_{1rr}-H_{2rr}=&-(A_{11}+A_{12}+A_{31}+A_{32})H^+\cdot\vec{a}_\phi\\&-(A_{21}+A_{41})H^-\cdot\vec{a}_\phi\\&-(A_{12}+A_{32})H^+\cdot\vec{a}_\phi\end{aligned} \tag{17}$$

where, H^+, H^- is given by

$$H^+=Y_0\frac{e^{-j\beta d}}{b}\vec{a}_\phi \tag{18}$$

$$H^-=-Y_0\frac{e^{j\beta d}}{b}\vec{a}_\phi \tag{19}$$

Substitute eq. (6) ~ eq. (9) and eq. (14) ~ eq. (16) to eq. (2) and substitute eq. (10) ~ eq. (13) and eq. (17) ~ eq. (19) to eq. (3) to obtain the expressions of P_r and M_ϕ as

$$\begin{bmatrix}P_r\\M_\phi\end{bmatrix}=C\begin{bmatrix}a_{11}&a_{12}\\a_{21}&a_{22}\end{bmatrix}^{-1}\begin{bmatrix}\frac{2j\sin\beta d}{b}\\-\frac{2\cos\beta d}{b}\end{bmatrix} \tag{20}$$

where,

$$a_{11}=\frac{2w\sin\beta de^{-j\beta d}}{Pb^2}-\frac{jw}{Pb^2}(1-e^{-2j\beta d})-\frac{1}{a_e\varepsilon}$$

$$a_{12}=-2j\frac{w\mu_0 Y_0\cos\beta d}{Pb^2}e^{-j\beta d}-\frac{jw\mu_0 Y_0}{Pb^2}(1-e^{-2j\beta d})$$

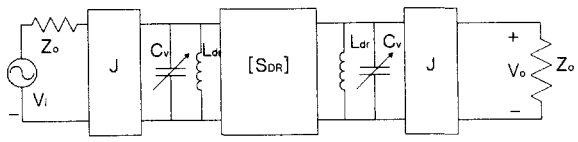

Fig. 4. Equivalent circuit of Fig. 2.

$$\begin{aligned}a_{21}&=\frac{2w\sin\beta de^{-j\beta d}}{Pb^2}+\frac{jw}{Pb^2}(1+e^{-2j\beta d})\\a_{22}&=-Y_0\frac{2jw\mu_0\cos\beta de^{-j\beta d}}{Pb^2}\\&\quad-Y_0\frac{jw\mu_0}{Pb^2}(1+e^{-2j\beta d})-\frac{1}{a_m Y_0}\end{aligned}$$

and, $\varepsilon=\varepsilon_r\varepsilon_0$, ε_r is the permittivity of the DR.

Because we can calculate electric field radiated by dipole moments, the scattering parameters can also be expressed as

$$\begin{aligned}S_{21}&=S_{12}=(A_{11}+A_{12}+A_{31}+A_{32})e^{-2j\beta l}\\&=\left(\frac{2w\sin\beta d}{Pb}P_r-2j\frac{w\mu_0 Y_0\cos\beta d}{Pb}M_\phi\right)e^{-2j\beta l}\end{aligned} \tag{21}$$

$$S_{11}=S_{22}=-e^{-2j\beta l}-S_{21} \tag{22}$$

Fig. 4 is the equivalent circuit of Fig. 2. J denotes the low coupling of the input/output section, C_v is the equivalent variable capacitance of the varactors and L_r denotes admittance of DRs which this admittance is given as

$$Y=-jY_0\cot\beta l \tag{23}$$

where, l is the length of the DR.

The coupling windows is now represented as generalized scattering parameters, $[S_{DR}]$, obtained by eq. (22). Transmission coefficient calculation of circuits shown in Fig. 4 enables us coupling factors calculation.

The comparisons between calculated coupling factor and measured one are presented in Fig. 5 and Fig. 6. The DR considered in this paper has physical dimensions and property as following :

Radius of inner conductor, $a=2.75$ mm
Radius of outer conductor, $b=8$ mm
Permittivity, $\varepsilon_r=37$

Fig. 5 shows the comparison when the resonator is composed of only DR whereas Fig. 6 shows the comparison when the resonator is composed of DR connected with 39 pF C and 3 pF C using leads. There are very close agreements between calculated results and measured one.

By comparison between calculated coupling factor of coupling windows and the desired values expressed in terms of low-pass proto type[1], the optimized coupling windows can be designed.

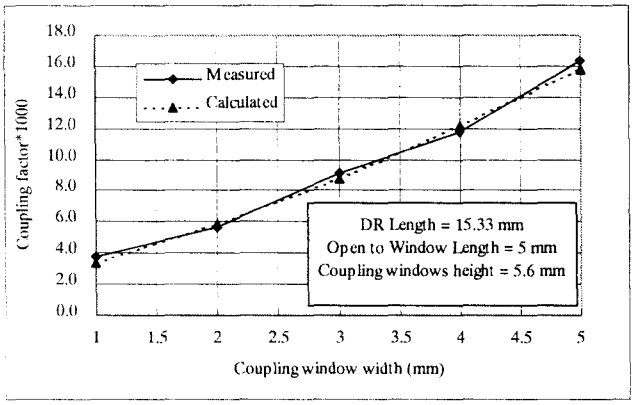

Fig. 5. Coupling factor comparison between measured and calculated : resonator is composed of only DR.

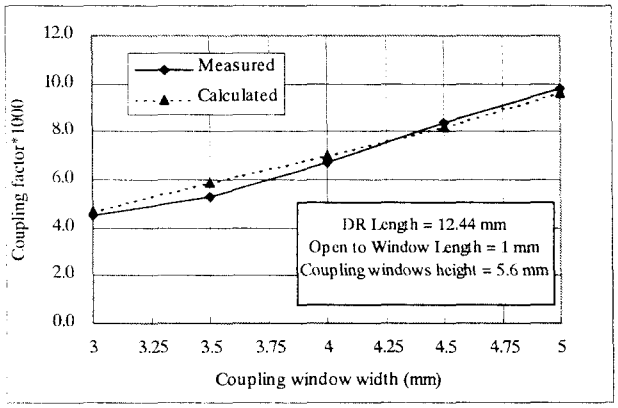

Fig. 6. Coupling factor comparison between measured and calculated : resonator is composed of DR connected with 39 pF C and 3 pF C using leads.

Ⅲ. Design of Input/Output Section

As shown in Fig. 1, the input/output coupling is realized by virtue of series lumped L, C elements. The external Q is selected as design parameters[1]. To minimize passband insertion loss, the resonator must be operated at its' highest Q region. To satisfy this requirement, DR must have largest length which is equivalent to lowest varactor capacitance[7]. Eq. (24) is the external Q expression[1] of suggested structure.

$$Q=\frac{bG_A}{B^2} \tag{24}$$

where, G_A is the admittance of source/load circuits,

$$b=\frac{Y_0}{2}\theta\csc^2\theta+wC_v,\quad B=\left(wL_{01}-\frac{1}{wC_{01}}\right)^{-1} \text{ and } \theta=\beta l.$$

C_{01}

If external Q requirement over tuning frequency range ,which is expressed in terms of low pass proto type[1], can be satisfied by changing and L_{01}, the DR length, l, can be determined to give highest resonator Q. Note that if coupling section is composed of only C or L, the external Q requirement cannot be satisfied unless DR length, l, become shorten[1]. If DR length is selected so that resonator can be operated at highest Q region, we can satisfy not only constant bandwidth requirement but also minimum passband insertion loss requirement. Further discussion associated with this will be presented with practical example.

Ⅳ. Practical Example

A varactor tuned RF tunable bandpass filter has been designed and constructed to the following specification :

Frequency : 800 MHz~900 MHz
Passband bandwidth : 10 MHz (W = 1.2 %)
Type : 5 sections, 0.01 dB ripple Chebyshev

The varactors used are BB535 RF Variable Capacitance Diodes[1)2)]. Fig. 7 shows the calculated coupling factors between 1 st resonator and 2 nd resonator vs frequency axis. Three straight lines are calculated from low-pass proto type in cases of 9.8 MHz, 10 MHz and 10.2 MHz bandwidths. Three curved

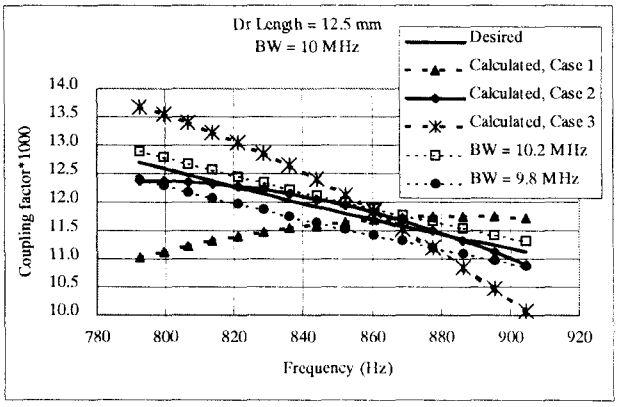

Fig. 7. The coupling factor vs frequency axis.
Case 1 : SW = 6 mm, w = 1.8 mm, l = 6.15 mm
Case 2 : SW = 6.9 mm, w = 4.4 mm, l = 6.15 mm
Case 3 : SW = 8 mm, w = 4.5 mm, l = 7.5 mm
(See Fig. 1 for SW, w, l).

[1] Phillips Semiconductor, Sunnyville, CA.

[2] Device parameters based on manufacturer supplied data.

Table 1. The position and size of coupling windows.

Coupling windows	SW	w	l	BW variation
Between 1 st resonator to 2 nd resonator	6.9 mm	4.4 mm	6.15 mm	less than ±0.15 MHz
Between 2 nd resonator to 3 rd resonator	7.8 mm	2.3 mm	6.15 mm	less than ±0.1 MHz

Note : the coupling windows are symmetrical.

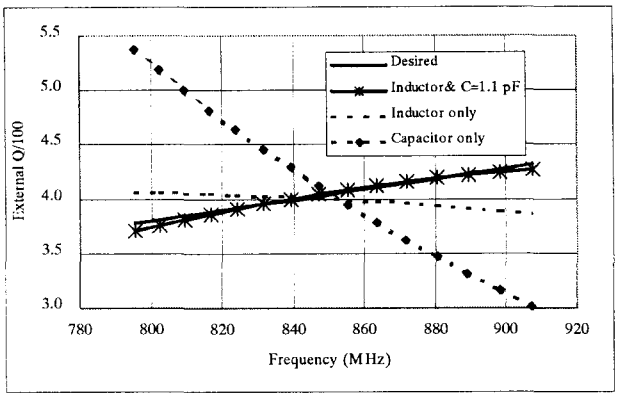

Fig. 8. The external Q vs frequency axis.

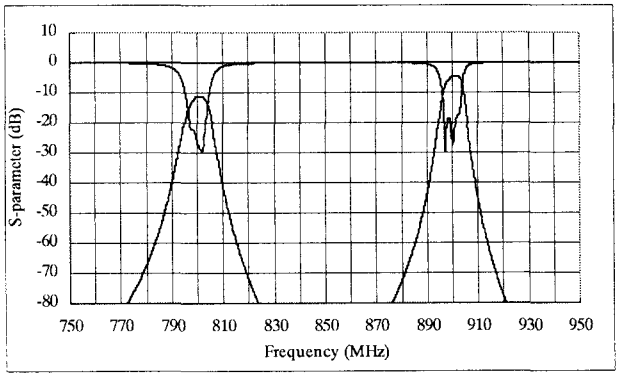

Fig. 9. Calculated scattering parameters of 5 sections varactor-tuned RF bandpass filter.

lines are calculated by presented method. Case 2 would be optimally designed case because this case shows most close to the desired values for 10 MHz bandwidths within tuning frequency range. The passband bandwidth variation is predicted less than ±0.15 MHz. Also, it is predicted that the passband bandwidth will be narrower at low(about 800 MHz) and high(about 900 MHz) frequency region compared with average one and will be broader at mid(about 850 MHz) frequency region. Similarly, the position and size of coupling windows are determined as shown in Table 1.

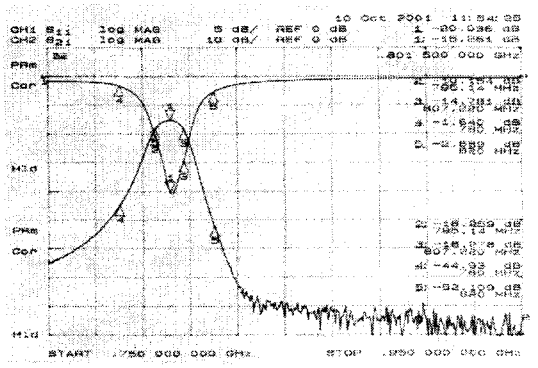

(a)

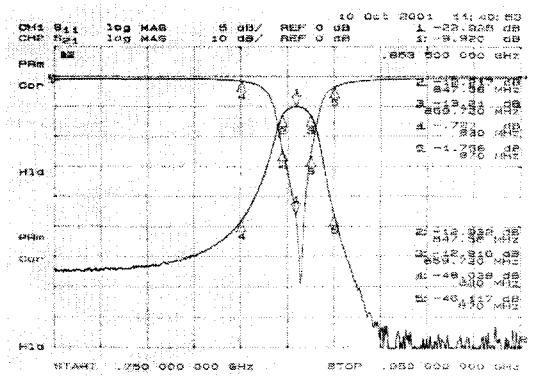

(b)

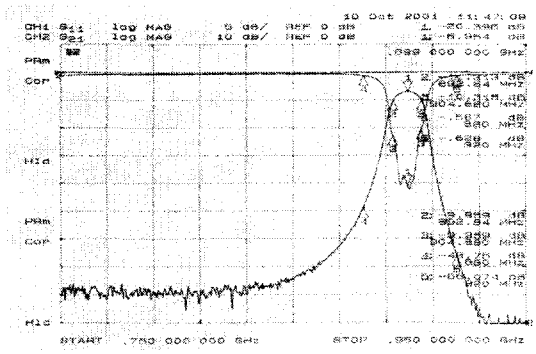

(c)

Fig. 10. Experimental results.
(a) Center frequency = 800 MHz, 3 dB passband bandwidth = 12.08 MHz, Insertion loss = 15.3 dB
(b) Center frequency = 850 MHz, 3 dB passband bandwidth = 12.16 MHz, Insertion loss = 9.9 dB
(c) Center frequency = 900 MHz, 3 dB passband bandwidth = 12.04 MHz, Insertion loss = 7.0 dB

Fig. 8 shows external Q variation vs frequency axis as a function of coupling method with largest DR length. The desired values are calculated using low pass proto type expressions[1]. It can be concluded that coupling method using series lumped L, C elements satisfy not only the constant bandwidth requirement but also minimum passband loss requirement.

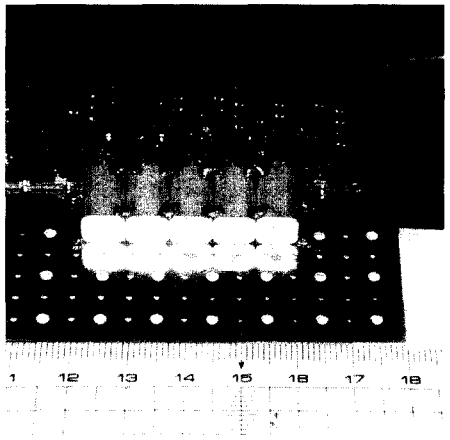

Fig. 11. Photograph of the experimental varactor-tuned filter.

The overall transmission coefficient, S_{21}, can be calculated because scattering parameters of the each section has been obtained.

Fig. 9 shows the calculated overall transmission coefficient. Constant bandwidths with relatively low passband loss are predicted within designed tuning frequency range. Note that our design example is 5 sections and fractional bandwidth is only 1.2 %. Because passband loss will (exponentially) increase proportional to the number of poles or inverse proportional to the fractional bandwidths[1],[2], it can be concluded that designed filter shows relatively low passband loss mostly due to loss of varactor diode. This result can be implemented because resonator is enforced so that is operated at highest Q region. However, for compensating purpose RF equalizer[9] can be applied.

Fig. 11 shows a photograph of the experimental varactor-tuned RF bandpass filter. Fig. 10 shows experimental results. The 3 dB passband bandwidth variation was 0.12 MHz (less than 1 %) within designed frequency range. The passband loss was 15 dB~7 dB. These results agree well with predicted ones.

V. Conclusion

A novel varactor-tuned bandpass filter is proposed and design method for optimum response is discussed. Experimental results agree well with the predicted ones. The proposed design method enables one to design a varactor-tuned bandpass filters with constant passband bandwidth and relatively low passband insertion loss.

References

[1] G. L. Matthaei, L. Young, and E. M. T. Jones, *Microwave Filters, Impedance-Matching Networks, and Coupling Structures*. Norwood, MA: Artech House, 1980.

[2] I. C. Hunter and J. D. Rhodes, "Electronically tunable microwave bandpass filter", *IEEE Trans. Microwave Theory Tech.*, vol. MTT-30, pp. 1354-1360, Sept. 1982.

[3] M. Makimoto and M. Sagawa, "Varactor tuned bandpass filters using microstrip-line ring resonators", in *IEEE MTT-S Int. Microwave Symp. Dig.*, May 1986, pp. 411-414.

[4] Y.-H. Shu, J. A. Navarro, and K. Chang, "Electronically switchable and tunable coplanar waveguide-slotline bandpass filters", *IEEE Trans. Microwave Theory Tech.*, vol. 39, pp. 548-554, Mar. 1991.

[5] Andrew R. Brown and Gabriel M. Rebeiz, "A varactor-tuned RF filter", *IEEE Trans. Microwave Theory Tech.*, vol. 48, pp. 1157-1160, July 2000.

[6] Y. Ishikawa, T. Nishikawa, T. Okada, S. Shinmura, Y. Kamado, F. Kanaya, and K. Wakino, "Mechanically tunable MSW bandpass filter with combined magnetic units", in *IEEE MTT-S Int. Microwave Symp. Dig.*, 1990, pp. 143-146.

[7] R. E. Collin, *Foundation for microwave engineering*, Second Edition, McGraw-Hill, Inc., 1992.

[8] H. A. Bethe, "Theory of Diffraction by Small Holes", *Phys. Rev.*, vol. 66, pp. 163-182, 1944.

[9] Hee-Young Hwang, Jung-Seong Jung and Sang-Won Yun, "An RF amplitude equalizer; improved passband flatness of a bandpass filters", *Journal of the Korea Electromagnetic Engineering Society*, vol. 1, No. 1, May 2001.

[10] S. B. Cohn, "The electric polarizability of apertures of arbitrary shape", *Proc. IRE* 40, pp. 1069-1071, Sep. 1952.

Byung-Wook Kim

received the B.S. and M.S. degrees from the Department of Electronic Engineering, Sogang University, Seoul, Korea, in 1994 and 1996, respectively. From 1996 to May 2001, he worked as research engineer in Korea research institute of standards and sciences(KRISS). Since May 2001, he has been with a degree of Ph.D. in electronic engineering from Sogang University. His research interests include microwave and millimeter- wave devices and numerical analysis.

Du-Il Yun

received the B.S. degree from the Department of Electronic Engin- eering, Sogang University, Seoul, Korea, in 2001. Since 2001, he has been with a degree of M.S. in electronic engineering from Sogang University. His research interests include microwave filters.

Sang-Won Yun

received the B.S. and M.S. degrees from Seoul National University, Seoul, Korea, in 1977 and 1979, respectively, and the Ph.D. degree from Univ. of Texas at Austin in 1984. Since 1984, he has been a Professor in the Department of Electronic Engineering, Sogang University, Seoul, Korea. From January 1988 to December 1988, he was a Visiting Professor at the University of Texas Austin. His research interests include microwave and millimeter-wave devices and circuits.